Proceedings of the 33rd European Safety and Reliability Conference (ESREL 2023)
Edited by Mário P. Brito, Terje Aven, Piero Baraldi, Marko Čepin and Enrico Zio
 Published by Research Publishing, Singapore.
doi: 10.3850/978-981-18-8071-1_P123-cd

Reliability analysis of flexural subassemblies under ultra-high and low cycle fatigue based on Monte-Carlo method

Yongtao Bai

School of Civil Engineering, Chongqing University, China. E-mail:bai.yongtao@cqu.edu.cn

Cheng Xie*

School of Civil Engineering, Chongqing University, China. E-mail:xiecheng@stu.cqu.edu.cn

Julio Flórez-López

School of Civil Engineering, Chongqing University, China. E-mail: j.florezlopez@cqu.edu.cn

Abstract: Flexural subassemblies are widely used in building structures (beams and columns) and bridges. Structures in earthquake prone areas are not only subjected to ultra-low cycle (<100 cycles) fatigue (ULCF) load caused by earthquake action, but also experience ultra-high cycle (>10 million cycles) fatigue (UHCF) load during their service life, such as vehicle load and wind load. This paper first introduced a method, that is ultra-high cycle fatigue pre-damage and ultra-low cycle fatigue damage (UHCF_PreD-ULCF_D) criteria based on lumped damage mechanics, to model the damage state of flexural subassemblies under combined fatigue loading. The fatigue loading test data of three flexural subassemblies were referred to verify the accuracy of the model; Then, the reliability analysis and computing process of flexural subassemblies under fatigue damage state based on Monte Carlo method were established; Finally, the reliability of flexural subassemblies was analyzed under the uncertainty of material constant, loading cycle and lateral force. The results showed that UHCF_PreD-ULCF_D models of the flexural subassemblies not only achieved high accuracy, but also greatly improved the computing speed and convergence when calculating the UHCF and ULCF loading responses. The efficient method of calculating structural damage state was well applicable to the Monte Carlo method for reliability analysis. The reliability analysis program proposed for flexural subassemblies could consider the uncertainty of external loads and material defects well, compute the failure probability of the components efficiently, and calibrate the critical value of the damage variable of the theoretical model corresponding to structural failure.

Keywords: Structural reliability, flexural subassemblies, ultra-high cycle fatigue, ultra-low cycle fatigue, lumped damage mechanics, Monte Carlo method, Mathematical methods, Uncertainty analysis

1. Introduction

For complex steel structures and composite structures, e.g., railway bridge, turbine and offshore structure, they are faced with damage or failure due to cyclic load or destructive earthquake during their service life, which is considered to be caused by fatigue effect. It is estimated that 90% of the damage of engineering structures and components can be attributed to fatigue effects. Eurocode-3 (e.g., Anderson, 2003) first defined fatigue failure as the damage in progressive crack growth process caused by fluctuating stress of structural members. For high cycle fatigue assessment of steel structures, the most commonly method was based on the S-N curve recorded in Eurocodes, which was empirical and lack of damage evolution process, resulting in not accurate enough estimation (e.g., Bazan et al., 2019). Many steel structures normally operate under complex loadings coupling with uncertainties originating from multiple sources, including material variability, load variation and geometrical uncertainty (e.g., Niu et al., 2019). To this end, Sankararaman et al. (2011) presented a methodology for uncertainty

quantification and model validation in fatigue crack growth analysis.

Noted that above resolutions were from micro perspective, difficulties in fatigue assessment of steel structures at the macro level remain unsolved. Flórez-López et al. (2015) proposed the lumped damage mechanics based on the phenomenon that plastic hinges intensively developed on the nodes of flexural subassemblies, which has been proved to be able to interpret the fatigue macro-damage of steel structures under cyclic loads accurately and efficiently by Bai et al. (2021). Also, structures in earthquake prone areas are not only subjected to LCF loading caused by earthquake action, but also experience HCF loading during their service life, such as vehicle load and wind load, so the existing limitation is that the combined models of macro structures under LCF and HCF have rarely been established. Bai et al. (2022) presented a framework combining HCF and LCF macro approaches for evaluating the remaining-life of high-rise steel buildings based on fatigue damage propagation in local beam-to-column connections. Nevertheless, another limitation is that the probability of remaining-life in Bai's model could not be calculated due to the lack of uncertainties. For the reliability method to estimate the failure probability, the Bayesian approach (e.g., Straub 2009; Dang et al. 2022), active learning method (e.g., Moustapha et al. 2022), probability density evolution method (e.g., Li, 2016) and Monte Carlo (MC) simulation (e.g., Su et al. 2022; Papaioannou et al. 2015) provides different perspective. Although the MC viewpoint is concise and frequentist (e.g., Owen, 2019), it is still a highly effective tool for non-linear and discontinue failure probability estimation (e.g., Rubinstein, 2016). Furthermore, the ultra-high cycle fatigue pre-damage and ultra-low cycle fatigue damage (UHCF_PreD-ULCF_D) model proposed could contribute to the application of MC simulation on reliability of flexural subassemblies with less time assuming.

This paper extends the combined HCF and LCF fatigue probability model to overcome these limitations. The work is structured as follows: in Section 2, HCF and LCF damage criteria based on lumped damage mechanics are introduced, to model the damage state of flexural subassemblies under combined fatigue loading; Section 3 elaborates a framework for fatigue probability model by taking uncertainty of material constant, loading cycle and lateral force into consideration; in Section 4, results and discussions are given; finally, conclusions are drawn in Section 5.

2. Model of UHCF_PreD-ULCF_D

Ultra-high cycle fatigue is considered to be the condition that experiences more than 10 million fluctuating stress loading within yield stress during their service life, usually occurring on flexural subassemblies of steel bridge (Fig. 1a) and high-rise building (Fig. 1b) subjected to vehicles or wind load. In contrast, ultra-low cycle fatigue implies that the number of loading cycle is only dozens, but the zone of steel flexural subassemblies prone to fatigue firstly enters into the plastic stage and then produces more cumulative plastic rotation under earthquake motion. As shown in Fig. 1, under ultra-high cycle fatigue, the maximum elastic stress fiber of steel component keeps in the process of crack initiation with cycles increase, which is quantified by pre-damage variable ω_H. For the comprehensive model of UHCF_PreD-ULCF_D representing the routine high cycle fatigue loading plus the accidental destructive loading, the latter contributes to accelerating pre-damage process, and then cracks initiating and propagating. The damage state, that is indeed crack propagation, is defined as variable $\boldsymbol{d}$. When d=1.0, the flexural subassemblies mean completely failed. For us, instantaneous collapse damage of structure is absolutely prevented, so the damage variable is actually not available to 1.0, and the critical value of d_{cr} corresponding to structural failure should be determined.

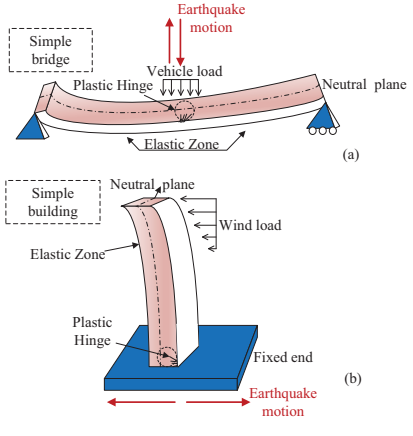

Fig. 1. (a) Flexural subassemblies of steel bridge; (b) flexural subassemblies of high-rise building;

2.1 *Pre-damage law*

For UHCF_PreD model, the well-known Basquin law is firstly used to calculate life cycle N of metal materials under constant elastic stress radiation, as shown in the following formula:

$$N_{cr} = \left(\frac{\Delta\sigma}{\sigma_f} \right)^{\gamma} \tag{1}$$

Where, $\Delta\sigma$ is the amplitude of the elastic stress, and σ_f and γ are the material parameters.

For flexural subassemblies (such as Fig. 1a and b), the fatigue damage is concentrated at the inelastic hinge, so the stress amplitude at any fiber of the section can be determined as follows:

$$\Delta\sigma(z) = \frac{\Delta m \cdot z}{I} \tag{2}$$

Where, Δm is the bending moment amplitude, I is the section moment of inertia, and z is the distance between each fiber and the neutral axis. Therefore, for the UHCF_PreD model, the number of cycles of cracking initiation is expressed as follows:

$$N_{\mathrm{H}cr}(z) = \left(\frac{\Delta m \cdot z}{I\sigma_f} \right)^{\gamma} = \left(\frac{\Delta m}{M_f} \right)^{\gamma} \tag{3}$$

Where, $M_f = \dfrac{I\sigma_f}{z}$.

Therefore, the pre-damage variable ω_{H} is defined to quantify the stage of crack initiation under high cycle fatigue.

$$\omega_{\mathrm{H}} = N\left(\frac{\Delta m}{M_f} \right)^{-\gamma} \tag{4}$$

Where, N is the number of real loading cycles during its life, and ω_{H} pertains to [0, 1] that is, when ω_{H} is equal to zero, this is an ideal undamaged state for subassemblies; while, ω_{H} equal to one stands for the finish of crack initiation and the beginning of crack propagation, between both of which it is the stress-controlled cumulative cycles stage of crack initiation before damage.

Besides, when determining the pre-damage stage, crack initiation due to low cycle fatigue could not be neglected, noted that it is not stress-controlled but strain-controlled, resulting from the yielding of steel material. Herein, the well-known Coffin-Manson law is also referred as follows:

$$N = \left(\frac{\Delta\varepsilon_p}{\varepsilon_f} \right)^{\beta} \tag{5}$$

Where, $\Delta\varepsilon_p$ is the plastic strain amplitude. ε_f and β are the material parameters.

According to Palmgren-Miner criterion, fatigue fracture under different plastic strain amplitude values $\Delta\varepsilon_p{}^1$, $\Delta\varepsilon_p{}^2$, $\Delta\varepsilon_p{}^3$ occurs, when:

$$\sum \frac{N_k}{N_f^k} = 1 \tag{6}$$

Where $N_f{}^k$ is the number of cycles of fracture when the strain amplitude is $\Delta\varepsilon_p{}^k$, and N_k is the actual number of cycles under this amplitude.

Similar with Eq. (3), for the subassemblies with plastic hinge subjected to low cycle fatigue, the plastic strain amplitude of the fiber at the distance z from the neutral axis can be approximated as:

$$\Delta\varepsilon_p = \frac{z\Delta\phi_p}{L_p} \tag{7}$$

Where $\Delta\phi_p$ is the periodic amplitude of plastic rotation and L_p is the equivalent plastic length. Therefore, the number of cycles $N_{\mathrm{L}cr}$ of crack initiation is expressed as follows:

$$N_{\mathrm{L}cr}(z) = \left(\frac{z \cdot \Delta\phi_p}{L_p\varepsilon_f} \right)^{\beta} = \left(\frac{\Delta\phi_p}{\phi_f} \right)^{\beta} \tag{8}$$

Where, the parameter ϕ_f is the plastic rotation amplitude required to produce cracks in the plastic hinge region at the end of the first cycle. When the section is cracked, $N_{\mathrm{L}cr}(z)$ decreases with the upward movement of the neutral axis. It is considered that the hinge is no longer plastic but inelastic after the crack occurs.

Based on lumped damage mechanics, it is considered that all inelastic effects, including plastic deformation and fatigue pre-damage, are concentrated at the zero-length hinge. The pre-damage variable from the part of low cycle fatigue ω_{L} is also introduced to measure whether cracks occur in the cross-section of the member. When the sum of ω_{L} and ω_{H} less than 1.0, there is no crack in the section; When ω equals to 1.0, the section produces tiny cracks and the subassemblies enter into a damaged state.

$$\omega_{\mathrm{L}} = \frac{p}{p_{cr}} = \frac{p}{2\Delta\phi^p}\left(\frac{\Delta\phi^p}{\phi_f^p} \right)^{-\beta} = N\left(\frac{\Delta\phi^p}{\phi_f^p} \right)^{-\beta} \tag{9}$$

$$\{\omega\}_{\mathrm{b}} = \{\omega_{\mathrm{H}}\}_{\mathrm{b}} + \{\omega_{\mathrm{L}}\}_{\mathrm{b}} = \begin{bmatrix} \omega_{\mathrm{H}i} \\ \omega_{\mathrm{H}j} \end{bmatrix} + \begin{bmatrix} \omega_{\mathrm{L}i} \\ \omega_{\mathrm{L}j} \end{bmatrix} \tag{10}$$

2.2 *Damage evolution law*

As the flexural subassemblies of infrastructure are designed as elastic state during the daily operation phase, the plastic damage only attributes to low cycle fatigue, represented by d_L. The derivation is as follows:

$$N=\left(\frac{(1-d_L(N))^{\alpha}\Delta\phi^{p}}{\phi_f^{p}}\right)^{\beta} \quad if \quad N\geq N_{cr} \tag{11}$$

Where, α is a constant related to crack propagation.

$$\dot{d_L}=-\left(\frac{1-d_L(N)}{\beta\alpha}\right)\left(\frac{(1-d_L(N))^{\alpha}\Delta\phi^{p}}{\phi_f^{p}}\right)^{-\beta} \tag{12}$$

Also, it is considered that the effect of high cycle stress fatigue on crack propagation could be interpreted by energy release rate, and described by Dowling and Begley evolution laws. They are as follows:

$$\dot{d_H}=Q\left(\Delta G(d_H)\right)^{R} \tag{13}$$

$$G=\frac{L\langle m\rangle_{+}^{2}}{2EI\left(1-d_H\right)^{2}}\ , \qquad \langle m\rangle_{+}=\begin{cases}0 & if\ m<0\\ m & if\ m\geq 0\end{cases} \tag{14}$$

Where Q and R are model parameters. ΔG is the amplitude of the energy release rate at the damaged hinge of each cycle. L is the length of bar element.

Above equation could be achieved by numerical iteration based on commercial software ABAQUS Standard via the UEL option. Besides, the Monte Carlo simulation framework of UHCF_PreD-ULCF_D model considering uncertainties would be established, and the validation case would be carried out also in the following sections.

3 UHCF_PreD-ULCF_D reliability model

In this paper, framework of UHCF_PreD-ULCF_D reliability model consists of four parts, that is kinematic equation, constitutive equation, equilibrium equation and Monte Carlo simulation. For this model, state variables from Eq. (1) ~ (14) belonging to three types of equation are summarized in Fig. 2.

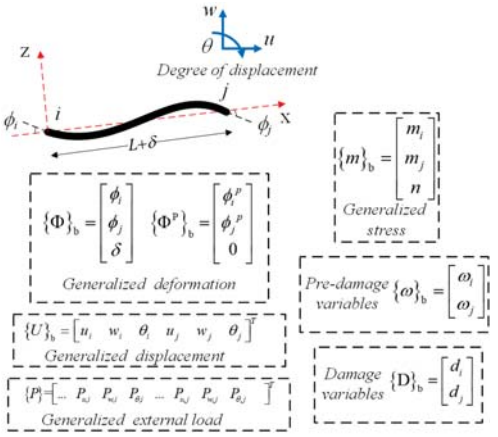

Fig. 2 Presentation of state variables

3.1. *Kinematic equation*

In the case of small deformation caused by fatigue loading, the relationship between generalized displacement and generalized deformation of any member b is:

$$\{\Phi\}_b=\left[B(U_b)\right]\{U\}_b$$

$$\left[B(U_b)\right]=\begin{bmatrix}0 & \cdots & \frac{\sin\alpha}{L} & -\frac{\cos\alpha}{L} & 1 & \cdots & -\frac{\sin\alpha}{L} & \frac{\cos\alpha}{L} & 0 & \cdots\\ 0 & \cdots & \frac{\sin\alpha}{L} & -\frac{\cos\alpha}{L} & 0 & \cdots & \frac{\sin\alpha}{L} & -\frac{\cos\alpha}{L} & 1 & \cdots\\ 0 & \cdots & -\cos\alpha & -\sin\alpha & 0 & \cdots & \cos\alpha & \sin\alpha & 0 & \cdots\end{bmatrix} \tag{15}$$

Where α is the inclination angle of member in the (X,Z) plane system, and L is the geometric length of member b. $[B(U_b)]$ is the conversion matrix.

3.2 *Equilibrium equation*

In this section, the internal force is solved through the generalized stress (the internal force of the node at the support is the reaction force of the support), and the relationship between the two is established through the equilibrium equation, that is, the relationship expression between the internal force of member b and the external force of two nodes:

$$\sum\left[B(U_b)\right]^{T}\{m\}_b-\{P\}=0 \tag{16}$$

3.3 *Constitutive equation*

(I) Elastic law

Under the condition of high cycle fatigue pre-damage, steel material is in the elastic stage, the relationship between stress and strain are linear, and there is no plastic deformation. The constitutive equation can be expressed as follows:

$$\{\Phi_h\}=[F_h]\{m_h\} \tag{17}$$

$$[F]=\begin{bmatrix} \frac{L}{3EI} & -\frac{L}{6EI} & 0 \\ -\frac{L}{6EI} & \frac{L}{3EI} & 0 \\ 0 & 0 & \frac{L}{AE} \end{bmatrix} \quad (18)$$

Where $[F]$ is the flexibility matrix, EI is the bending stiffness of member b, and AE is the tensile stiffness of member b.

(II) Inelastic law

The inelastic criteria considering stiffness degradation and crack closure are as follows:

$$\{\Phi\}_b-\{\Phi^p\}_b=\left[F^+(D)\right]\{m\}_b^+ \text{ or } \left[F^-(D)\right]\{m\}_b^- \quad (19)$$

$$\left[F^+(D)\right]=\begin{bmatrix} \frac{L}{3EI(1-h_i^+d_i^l-d_i^h)} & -\frac{L}{6EI} & 0 \\ -\frac{L}{6EI} & \frac{L}{3EI(1-h_j^+d_j^l-d_j^h)} & 0 \\ 0 & 0 & \frac{L}{EA} \end{bmatrix} \quad (20)$$

$$\left[F^-(D)\right]=\begin{bmatrix} \frac{L}{3EI(1-h_i^-d_i^l-d_i^h)} & -\frac{L}{6EI} & 0 \\ -\frac{L}{6EI} & \frac{L}{3EI(1-h_j^-d_j^l-d_j^h)} & 0 \\ 0 & 0 & \frac{L}{EA} \end{bmatrix} \quad (21)$$

Where, h_i^+, h_i^-, h_j^+, h_j^+ are the crack closure factors of i, j joints at the ends of the beam and column under the action of positive and negative bending moments, which are determined in accordance with Ref. [7].

The effective bending moment of the inelastic hinge is obtained using the strain equivalence assumption, so the yield function of the inelastic hinge determined by considering the effect of crack closure is:

$$f_i=\max\left(\frac{m_i}{1-h_i^+d_i^l-d_i^h}-c\phi_i^p,\frac{-m_i}{1-h_i^-d_i^l-d_i^h}+c\phi_i^p\right)-M_y\le 0 \quad (22)$$

$$f_j=\max\left(\frac{m_j}{1-h_j^+d_j^l-d_j^h}-c\phi_j^p,\frac{-m_j}{1-h_j^-d_j^l-d_j^h}+c\phi_j^p\right)-M_y\le 0 \quad (23)$$

Where, c is the yield strengthening coefficient, which is related to the material.

(III) Pre-damage evolution law

In the UHCF_PreD-ULCF_D model, the fatigue pre-damage state variable is used to measure whether the structure enters the damage state. Eq. (4), (9), (10) could be expressed as follows:

$$\dot{\omega}=\left(\frac{\Delta\phi_p}{\phi_f^p}\right)^{-\beta}+\left(\frac{\Delta m}{M_f}\right)^{-\gamma}= \left(\frac{p(N)-p(N-0.5)}{\phi_f^p}\right)^{-\beta}+\left(\frac{b(N)-b(N-0.5)}{M_f}\right)^{-\gamma} \quad (24)$$

$$\omega(N_{cr})=1$$

Where b(N) is accumulated bending moment after N times cycle. Noted that the increment step of cycles is 0.5 for convergency.

(IV) Damage evolution law

It can be seen from section 2.2 that the damage evolution law of high and low cycle fatigue:

$$\dot{d}=Q\left(\frac{G(N)-G(N-1)}{2}\right)^R-\frac{(1-d)}{\beta\alpha}\left(\frac{(1-d)^\alpha\left(p(N)-p(N-0.5)\right)}{\phi_f^p}\right)^\beta \quad (25)$$

$$if\ \ N\ge N_{cr}$$

When the structure enters the damage state, the damage factor is connected with the bending stiffness, and the flexibility matrix changes with the damage state, so as to realize the real-time update of the damage and flexibility matrix.

3.4 *Monte Carlo simulation*

Aimed at fatigue assessment on performance of bridges or buildings during their life, uncertainties generally including material constants, loading amplitude, and the number of cycles need to be considered. The UHCF_PreD-ULCF_D model combined with Monte Carlo simulation is presented in Fig. 3: Firstly, distribution types of random variables are determined and then the sample space Ω is established based on Python 3.6; Secondly, the corresponding parameters in UHCF_PreD-ULCF_D model are substitute as the random variables from sample space and then the force-displacement curve representing existing loading capacity and damage variables ω, d are obtained for each sample; Finally, by evaluating the residual loading capacity the failure probability of flexural subassemblies is calculated and the critical value of the damage variable of the theoretical model corresponding to structural failure is calibrated.

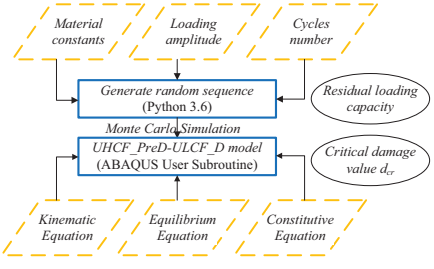

Fig.3 Framework of UHCF_PreD-ULCF_D reliability model

4 Result and discussions

4.1 *Validation of UHCF_PreD-ULCF_D model*

In order to verify the accuracy of *UHCF_PreD-ULCF_D model*, a series of tests for cantilever flexural subassemblies completed

by Zhou et al. (2013) were referred to, experimental details as shown in Fig. 4. Three specimens SP-3, SP-5, SP-7 (denoted by Zhou et al.) were selected to simulate by using *UHCF_PreD-ULCF_D model* based on ABAQUS Standard with UEL. The model parameters derived by Bai et al. (2021) were adopted in this simulation, that is: β=-1.783, α=0.45, R=-0.1, Q=0.0135, γ=-24, M_f =1150kN • m, M_y=307kN • m, ϕ_f=0.0326; crack closure effect h^-_i=0.3, h^+_i=1, h^-_j=0.3, h^+_j=1. Cyclic material Q345 model was adopted as shown in reference Zhou et al. (2013). Corresponding loading protocols were also in accordance with Zhou et al. (2013).

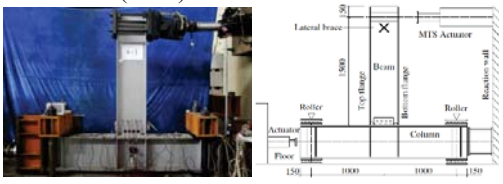

(a) General view (b) Components size

Fig. 4 Experimental details from Zhou (2013)

The load-displacements obtained from numerical simulation by *UHCF_PreD-ULCF_D model* were compared with that of experiment results from Zhou et al. (2013). It was shown in Fig. 5 that the numerical simulations for three specimens were in good agreement with experiment results (Zhou et al., 2013), including maximum and minimum load at each cycle and the degree of load degradation with cycle increase at maximum and minimum displacement. The only exception was the final failure stage, which was instantaneous unpredictable. Nevertheless, from the experiment result, we could find the failure value V_f was the half of ultimate loading capacity, and the simulation based on our theoretical model could describe the degradation of 40% of maximum value. Noted that in the following section η is defined as the residual capacity factor. Therefore, the critical loading capacity corresponding to structural failure could be preliminarily considered as $0.6V_0$, which could be used to calibrate the critical damage variable d_{cr} of our theoretical model.

$$\eta = V_f / V_0 \tag{26}$$

Where, V_0 is the loading capacity at the first cycle.

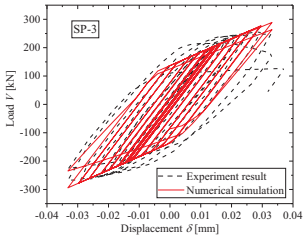

(a) SP-3

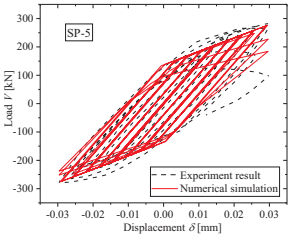

(b) SP-5

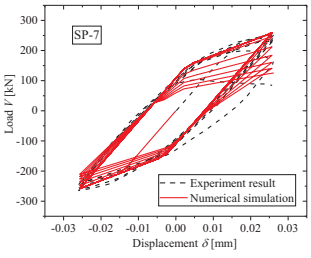

(c) SP-7

Fig. 5 Verification of the model proposed (Zhou et al., 2013)

4.2 *UHCF_PreD-ULCF_D probability model for SP-7*

(I) Effect of elastic modulus and loading amplitude

In this paper, the elastic modulus of column and the loading amplitude from the flexural subassembly SP-7 in 4.1 were considered as the uncertainties. According to actual conditions, distributions of elastic modulus and loading displacement amplitude were lognormal E~log$N$(12.2011, 0.0998)/10 and normal D~N(0.8, 0.25) × 1.75δ_y respectively and the sample space was defined as Ω(I). Above two random variables were applied in UHCF_PreD-ULCF_D probability model, and one thousand samples were calculated. The load-displacement curves of three random samples were shown in Fig. 6. Obviously, the loading capacity of flexural

assemblies were deeply influenced by elastic modulus of column and the loading amplitude due to accidental overload

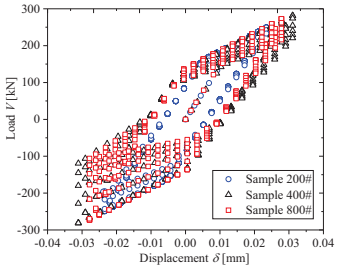

Fig. 6 Some samples with different elastic modulus and loading amplitude

(II) Effect of cycles number

Furthermore, the effect of high cycles number of daily uses at pre-damage stage on infrastructure also needs to be revealed. According to actual conditions, the cycles number of *UHCF_PreD* for the flexural subassembly SP-7 was considered as the uncertainty with uniform distribution $U\sim(10, 2000)\times 5000$, and the sample space was defined as Ω(II). This random variable was applied in UHCF_PreD-ULCF_D probability model, and one thousand samples were calculated. Three random samples were shown in Fig. 7 with respect to load-displacement curves. The preliminary judgement was that if no crack initiation before low-cycle overload, high cycles number was almost no impact on the loading capacity.

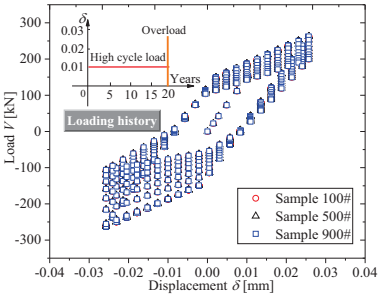

Fig. 7 Some samples with different high cycles number (loading history attached)

4.3 *Failure probability and damage calibration*

As section4.1 mentioned, the failure of flexural assemblies under fatigue loading is considered as the condition when the maximum loading capacity decrease 40% at the current cycle compared with the first cycle. From the sample space Ω(I) and Ω(II), the number of failed samples S_f is counted respectively, and then the failure probability P_f is calculated. Noted that under the destructive overload of ULCF, all samples from Ω(II), are failed, although the high cycle number varies from 5×10^4 to 10^7.

$$P_f(\mathrm{I})=\frac{S_f(\mathrm{I})}{S(\mathrm{I})}=0.231,\quad S\in\Omega(\mathrm{I}) \tag{27}$$

$$P_f(\mathrm{II})=\frac{S_f(\mathrm{II})}{S(\mathrm{II})}=1,\quad S\in\Omega(\mathrm{II}) \tag{28}$$

Besides, the damage variables $\boldsymbol{d}$ of all samples from Ω(I) and Ω(II) respectively are obtained and placed on the same figure with corresponding residual loading capacity factor $\boldsymbol{\eta}$, as shown in Fig. 8. It can be seen, when $\boldsymbol{\eta}$ =1, the damage variables are equal to zero, which represents the no damage state; more importantly, as data intensively distribute around $\boldsymbol{\eta}$ =0.4 and $\boldsymbol{d}$ =0.65, we could determine the critical damage variable of the UHCF_PreD-ULCF_D reliability model corresponding to failure as 0.65.

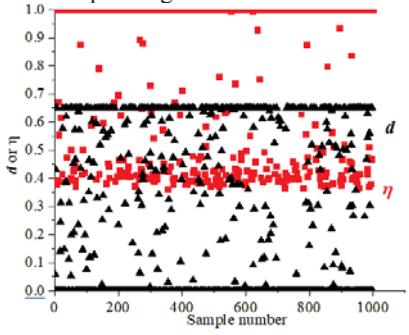

(a) Samples with different elastic modulus and loading amplitude

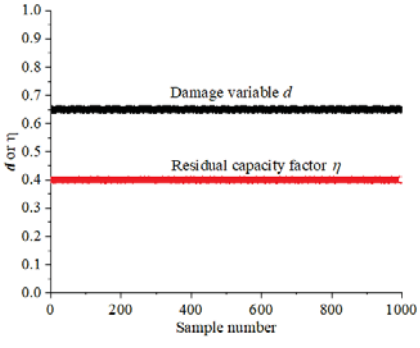

(b) Samples with different high cycles number

Fig. 8 The relevance between the damage variables and residual loading capacity factor

5 Conclusions

In this paper, the UHCF_PreD-ULCF_D

reliability models for the steel flexural subassemblies were proposed. Also, the accuracy and effectiveness of this theoretical model were verified via real experiment results and two groups of Monte Carlo simulation. The following conclusion could be obtained:

(1) For the steel flexural subassemblies subjected to the high-cycle load and possible low-cycle overload or earthquake, the comprehensive model of UHCF_PreD-ULCF_D was presented based on lumped damage mechanics, and achieved by ABAQUS Standards with UEL subroutines. The accuracy of this numerical simulation was calibrated by real experiment results, and the theoretical model could also be verified by the consistency between experiments and simulations.

(2) Under the framework of Monte Carlo simulation, the UHCF_PreD-ULCF_D reliability models were proposed. It could be computed by combining the Python and ABAQUS. The effectiveness of this reliability model was verified by two groups of samples.

(3) The critical failure index of this UHCF_PreD-ULCF_D reliability model is defined, including the damage variables $\boldsymbol{d}$ and the residual loading capacity factor $\boldsymbol{\eta}$. The critical values corresponding failure of the two variables are determined, that is, when $\boldsymbol{\eta}$ =0.4 and $\boldsymbol{d}$ =0.65.

Acknowledgement

This study was partially supported by the National Key R&D Program of China under Grant No. 2022YFB2602700, the National Natural Science Fund for Excellent Young Scientists Fund Program, Scientific Research Fund of the Institute of Engineering Mechanics, CAE (2020EEEVL0413), the Fundamental Research Funds for the Central Universities (2022CDJKYJH052), and the Support Plan for Returned Overseas Scholars of Chongqing (cx2020022).

References

Anderson, D. (2003). *Eurocode 3 - Design of steel structures*. Springer Berlin Heidelberg.

Bazan, J., A.T. Beck, J. Florez-Lopez (2019). Random fatigue of plane frames via lumped damage mechanics. *Engineering Structures*, *182*, 301-315

Niu, X. P., R.Z. Wang, D. Liao, S. P. Zhu, X.C. Zhang, and B. Keshtegar (2021). Probabilistic modeling of uncertainties in fatigue reliability analysis of turbine bladed disks. *International Journal of Fatigue*, *142*, 105912.

Sankararaman, S., Y. Ling, and S. Mahadevan (2011). Uncertainty quantification and model validation of fatigue crack growth prediction. *Engineering Fracture Mechanics*, *78*(7), 1487-1504.

Flórez-López, J., M.E. Marante, R. Picón (2015). *Fracture and damage mechanics for structural engineering of frames: state-of-the-art industrial applications*. S.l.: IGI Global.

Bai, Y.T., Y. Ma, Q.S. Yang, J. Florez-Lopez, X.H. Li, F. Biondini (2021). Earthquake-induced damage updating for remaining-life assessment of steel frame substructure systems, *Mechanical Systems and Signal Processing*, *159*, 107782.

Zhou, X.H., Y. Bai, D. Nardi, Y. Wang, Y. Wang, Z. Liu, R. Picon, J. Florez-Lopez (2022). Damage evolution modeling for steel structures subjected to combined high cycle fatigue and high-intensity dynamic loadings, *International Journal of Structural Stability and Dynamics*, 2240012.

Straub, D. (2009). Stochastic modeling of deterioration processes through dynamic Bayesian networks. *Journal of Engineering Mechanics*, *135*(10), 1089-1099.

Dang, C., M. A. Valdebenito, M. G. Faes, P. Wei, and M. Beer (2022). Structural reliability analysis: A Bayesian perspective. *Structural Safety*, *99*, 102259.

Moustapha, M., S. Marelli, B. Sudret (2022). Active learning for structural reliability: Survey, general framework and benchmark. *Structural Safety*, 102174.

Li, J. (2016). Probability density evolution method: background, significance and recent developments. *Probabilistic Engineering Mechanics*, *44*, 111-117.

Su, Y. H., X.W. Ye, and Y. Ding (2022). ESS-based probabilistic fatigue life assessment of steel bridges: Methodology, numerical simulation and application. *Engineering Structures*, *253*, 113802.

Papaioannou, I., W. Betz, K. Zwirglmaier, and D. Straub (2015). MCMC algorithms for subset simulation. *Probabilistic Engineering Mechanics*, *41*, 89-103.

Owen, A.B. (2019). Comment: Unreasonable effectiveness of Monte Carlo. *Statist Sci*, *34*(1), 29 – 33.

Rubinstein, R.Y., D.P. Kroese (2016). *Simulation and the Monte Carlo method*. John Wiley and Sons.

Zhou H, Y. Wang, Y. Shi, J. Xiong, L. Yang (2013). Extremely low cycle fatigue prediction of steel beam-to-column connection by using a micro-mechanics based fracture model. *International Journal of Fatigue*, *48*, 90–100.